

The crystal structure, Hirshfeld surface analysis and energy frameworks of 2-[2-(methoxycarbonyl)-3,6-bis(methoxymethoxy)phenyl]acetic acid

Mustapha Tiouabi,^a Raphaël Tabacchi^a and Helen Stoeckli-Evans^{b*}

^aInstitute of Chemistry, University of Neuchâtel, Av. de Bellevaux 51, CH-2000 Neuchâtel, Switzerland, and ^bInstitute of Physics, University of Neuchâtel, rue Emile-Argand 11, CH-2000 Neuchâtel, Switzerland. *Correspondence e-mail: helen.stoeckli-evans@unine.ch

Received 11 May 2020

Accepted 15 June 2020

Edited by J. Ellena, Universidade de São Paulo, Brazil

Keywords: crystal structure; isocoumarin; hydrogen bonding; C—H··· π interactions; offset π – π interactions; supramolecular framework; Hirshfeld surface analysis; energy frameworks.

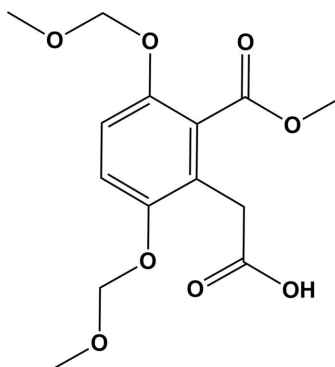
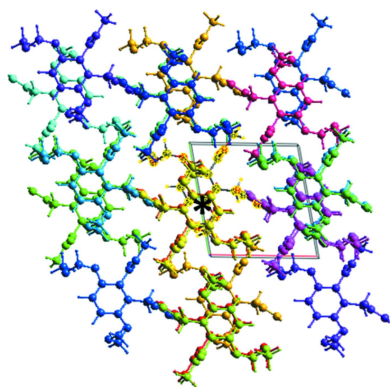
CCDC reference: 2009890

Supporting information: this article has supporting information at journals.iucr.org/e

In the title compound, C₁₄H₁₈O₈, (**1**), the methoxycarbonyl [–C(=O)OCH₃] and the acetic acid [–CH₂C(=O)OH] groups are inclined to the benzene ring by 79.24 (11) and 76.71 (13)°, respectively, and are normal to each other with a dihedral angle of 90.00 (13)°. In the crystal, molecules are linked by a pair of O–H···O hydrogen bonds forming the familiar acetic acid inversion dimer. The dimers are linked by two C–H···O hydrogen bonds and an offset π – π interaction [intercentroid distance = 3.6405 (14) Å], forming layers lying parallel to the (10 $\bar{1}$) plane. The layers are linked by a third C–H···O hydrogen bond and a C–H··· π interaction to form a supramolecular framework.

1. Chemical context

Isocoumarins are among the phytotoxins produced by the *Ceratocystis fimbriata* species. The latter are pathogenic agents responsible for the infections of coffee and plane trees (Gremaud & Tabacchi, 1994; Bürki *et al.*, 2003). The analysis of the culture medium of *Ophiostoma ulmi*, a pathogenic agent responsible for elm disease and classified in the family of *Ceratocystis*, enabled Michel (2001) to isolate sixteen metabolites including four isocoumarins without apparent toxicity and a new natural product, 3-methyl-3,5,8-trihydroxy-3,4-dihydroisocoumarin, found in the extract of diseased wood. Qualitatively, the latter is present in trace amounts; however, the toxicity of this metabolite is possible, since the activity is not necessarily proportional to the concentration.



The title compound (**1**), is a key intermediate for the proposed total synthesis of 3-methyl-3,5,8-trihydroxy-3,4-dihydroisocoumarin, and its synthesis is illustrated in Fig. 1 (Tiouabi, 2005). It was synthesized from hydroquinone (**1**), which was first brominated to give compound **2**. The latter was

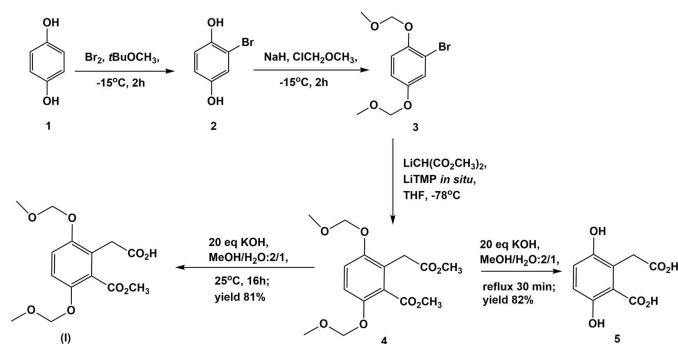


Figure 1
The reaction scheme resulting in the formation of the title compound, **I**.

then reacted with NaH and $\text{ClCH}_2\text{OCH}_3$ to give compound **3**, so protecting the hydroxyl groups. Reacting **3** with tetramethylpiperidine with *n*-butyllithium and $\text{CH}_2(\text{CO}_2\text{CH}_3)_2$ resulted in the formation of compound **4**. Finally **4** was reacted with various quantities of KOH in methanol/water (2:1) to give the title compound, **I**. The highest yield (81%) was obtained by reacting 20 equivalents of KOH in methanol/water (2:1) at 298 K under stirring for 16 h. Interestingly, the same reaction with reflux for 30 minutes yielded the diacid, 2-(methoxymethyl)-3,6-dihydroxybenzoic acid (**5**), with a yield of 82% (Fig. 1).

2. Structural commentary

The molecular structure of compound **I** is illustrated in Fig. 2. The methoxymethyl group (mean plane 1: C2/C7/O1/O2/C8; r.m.s. deviation = 0.009 Å) is inclined to the benzene ring by 79.24 (11)°. The plane of the acetic acid unit (mean plane 2:

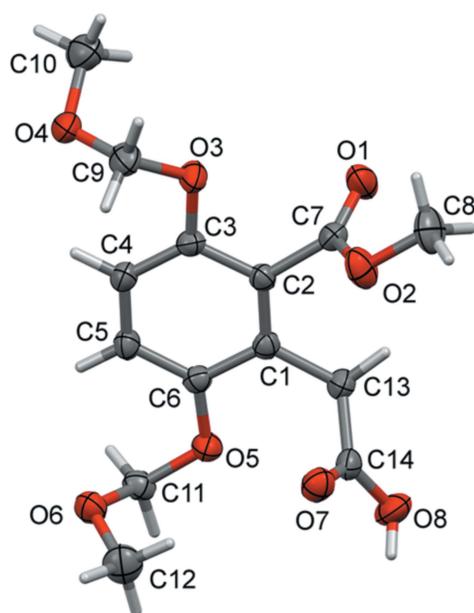


Figure 2
The molecular structure of compound **I**, with atom labelling. Displacement ellipsoids are drawn at the 50% probability level.

Table 1
Hydrogen-bond geometry (Å, °).

C_g is the centroid of the C1–C6 benzene ring.

$D-H\cdots A$	$D-H$	$H\cdots A$	$D\cdots A$	$D-H\cdots A$
O8–H8 \cdots O7 ⁱ	0.84	1.85	2.676 (2)	168
C9–H9B \cdots O6 ⁱⁱ	0.99	2.43	3.256 (3)	140
C11–H11A \cdots O1 ⁱⁱⁱ	0.99	2.38	3.366 (3)	175
C13–H13B \cdots O4 ^{iv}	0.99	2.50	3.421 (3)	155
C12–H12B \cdots C _g ^v	0.98	2.66	3.451 (3)	138

Symmetry codes: (i) $-x+1, -y+1, -z+1$; (ii) $x, y+1, z$; (iii) $-x, -y+1, -z$; (iv) $x+1, y, z$; (v) $-x, -y+1, -z+1$.

C13/C14/O7/O8; r.m.s. deviation = 0.014 Å) is inclined to the benzene ring by 76.71 (13)°. Planes 1 and 2 are normal to each other with a dihedral angle of 90.00 (13)°. The methoxymethoxy side chains (O3–C9–O4–C10 and O5–C11–O6–C12) are displaced to opposite sides of the benzene ring. They have twisted conformations as seen from the torsion angles given in Table 3.

3. Supramolecular features

In the crystal of **I**, molecules are linked by a pair of O–H \cdots O hydrogen bonds (O8–H8 \cdots O7ⁱ) forming an inversion dimer with an $R_2^2(8)$ ring motif (Fig. 3 and Table 1). The dimers are linked by two C–H \cdots O hydrogen bonds (C9–H9B \cdots O6ⁱⁱ and C11–H11A \cdots O1ⁱⁱⁱ) and offset π – π interactions between inversion-related benzene rings, so forming layers lying parallel to $(10\bar{1})$. The layers are linked by a third C–H \cdots O hydrogen bond (C13–H13B \cdots O4^{iv}) and a C–H \cdots π interaction to form a supramolecular framework (Table 1 and

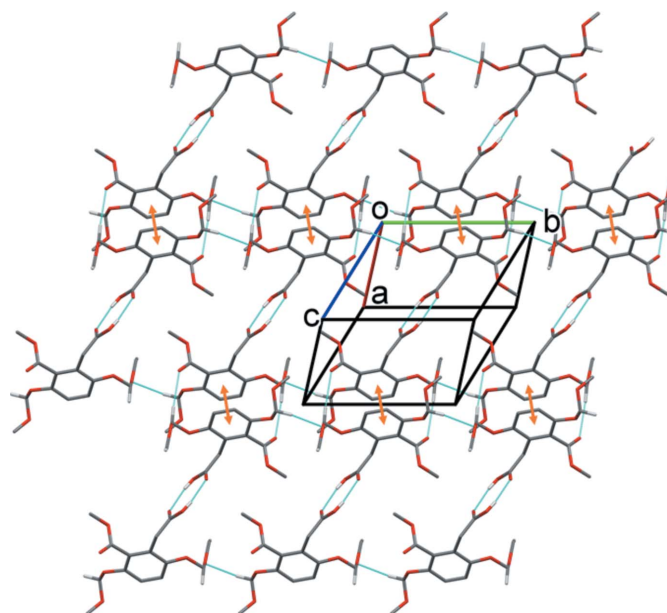
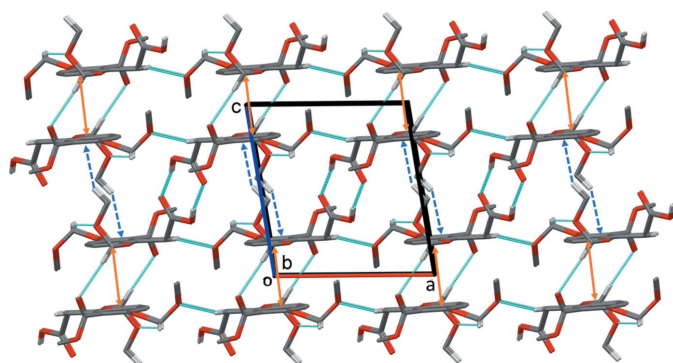


Figure 3
A view normal to plane $(10\bar{1})$ of the layer structure in the crystal of compound **I**. Hydrogen bonds (Table 1) are shown as dashed lines and offset π – π interactions as orange double arrows. For clarity, only the H atoms involved in the intermolecular interactions have been included.

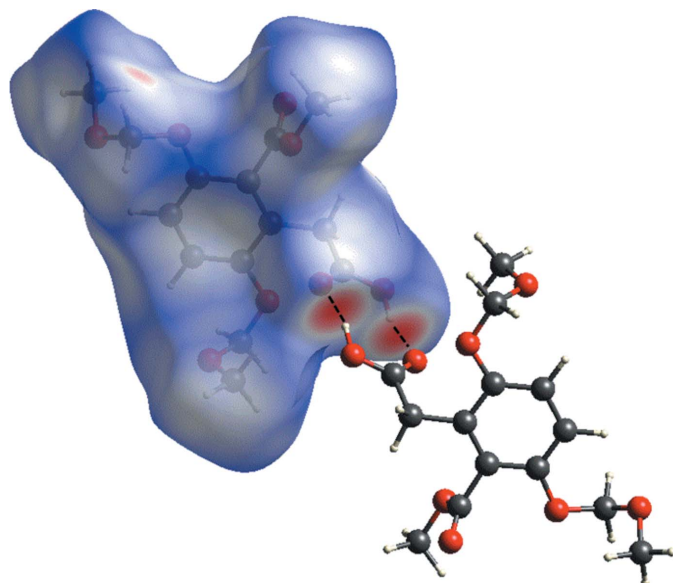

Figure 4

A view along the b axis of the crystal packing of compound **I**. The hydrogen bonds (Table 1) are shown as dashed lines. The offset π - π interactions are indicated by orange double arrows, and the $C-H \cdots \pi$ interactions by blue dashed arrows. For clarity, only the H atoms involved in the intermolecular interactions have been included.

Fig. 4). Details of the offset π - π interaction are as follows: $Cg \cdots Cg^{iii} = 3.6405(14) \text{ \AA}$, where Cg is the centroid of the C1-C6 benzene ring; interplanar distance = $3.5911(9) \text{ \AA}$; offset = 0.597 \AA ; symmetry code: (iii) $-x, -y + 1, -z$.

4. Hirshfeld surface analysis and two-dimensional fingerprint plots

The Hirshfeld surface analysis (Spackman & Jayatilaka, 2009), the associated two-dimensional fingerprint plots and the calculation of the energy frameworks (McKinnon *et al.*, 2007) were performed with *CrystalExplorer17.5* (Turner *et al.*, 2017), following the protocol outlined in the recent article by Tiekink and collaborators (Tan *et al.*, 2019). The Hirshfeld surface is colour-mapped with the normalized contact distance, d_{norm} , from red (distances shorter than the sum of the van der Waals radii) through white to blue (distances longer than the sum of


Figure 5

The Hirshfeld surface of compound **I** mapped over d_{norm} , in the colour range -0.6996 to 1.3669 a.u.

Table 2

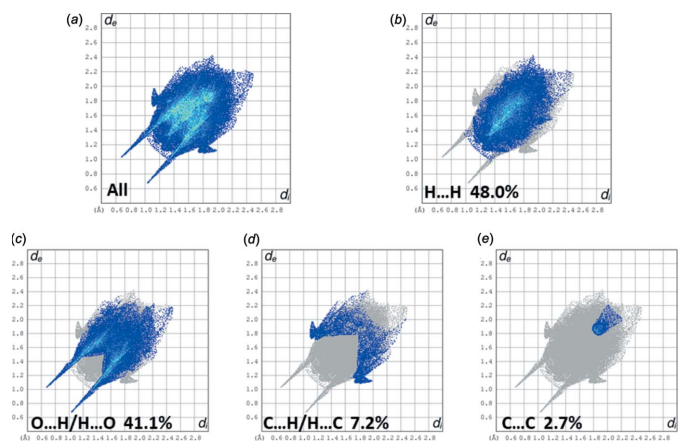
Short interatomic contacts (\AA)^a in the crystal of compound **I**.

Atom1	Atom2	Length	Length - VdW
O7	H8 ⁱ	1.850	-0.870
O7	O8 ⁱ	2.676	-0.364
O1	H11A ⁱⁱⁱ	2.379	-0.341
O6	H9B ^{vi}	2.432	-0.288
O4	H13B ^v	2.501	-0.219
H8	C14 ⁱ	2.703	-0.197
O5	H10C ⁱⁱⁱ	2.637	-0.083
C12	H9B ^{vi}	2.882	-0.018
O4	H8A ^v	2.723	0.003
O7	C8 ^{viii}	3.223	0.003
O7	H8B ^{viii}	2.726	0.006
O2	H8B ^{viii}	2.731	0.011
H8	H8 ⁱ	2.416	0.016
C2	H12B ^{vii}	2.932	0.032
O6	C9 ^{vi}	3.256	0.036
H8B	C14 ^{viii}	2.954	0.054
C9	H8A ^v	2.957	0.057
C1	H12B ^{vii}	2.968	0.068
C3	H12B ^{vii}	2.968	0.068
H10C	C11 ⁱⁱⁱ	2.969	0.069
H9B	H8A ^v	2.482	0.082

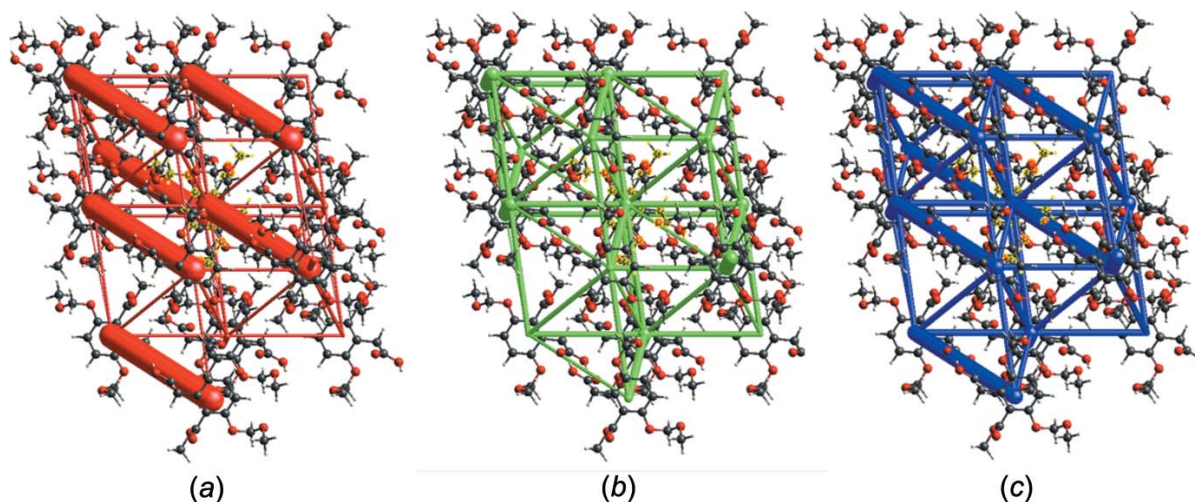
(a) Calculated using *Mercury* (Macrae *et al.*, 2020). Symmetry codes: (i) $-x + 1, -y + 1, -z + 1$; (iii) $-x, -y + 1, -z$; (v) $x - 1, y, z$; (vi) $x, y - 1, z$; (vii) $-x, -y + 1, -z + 1$; (viii) $-x + 1, -y + 2, -z + 1$.

the van der Waals radii). The energy frameworks (Turner *et al.*, 2015; Tan *et al.*, 2019) are represented by cylinders joining the centroids of molecular pairs using red, green and blue colour codes for the electrostatic (E_{ele}), dispersion (E_{dis}) and total energy (E_{tot}) components, respectively. The radius of the cylinder is proportional to the magnitude of the interaction energy.

A view of the Hirshfeld surface of **I** mapped over d_{norm} is shown in Fig. 5. The short interatomic $O \cdots H/H \cdots O$ contacts are indicated by the large red spots. Other $C-H \cdots O$ contacts are indicated by faint red spots. A full list of short interatomic contacts in the crystal of **I** are given in Table 2. The majority of the significant contacts are $O \cdots H$ and $C \cdots H$ contacts, as


Figure 6

(a) The full two-dimensional fingerprint plot for compound **I**, and fingerprint plots delineated into (b) $H \cdots H$ (48.0%), (c) $O \cdots H/H \cdots O$ (41.1%), (d) $C \cdots H/H \cdots C$ (7.2%) and (e) $C \cdots C$ (2.7%) contacts.

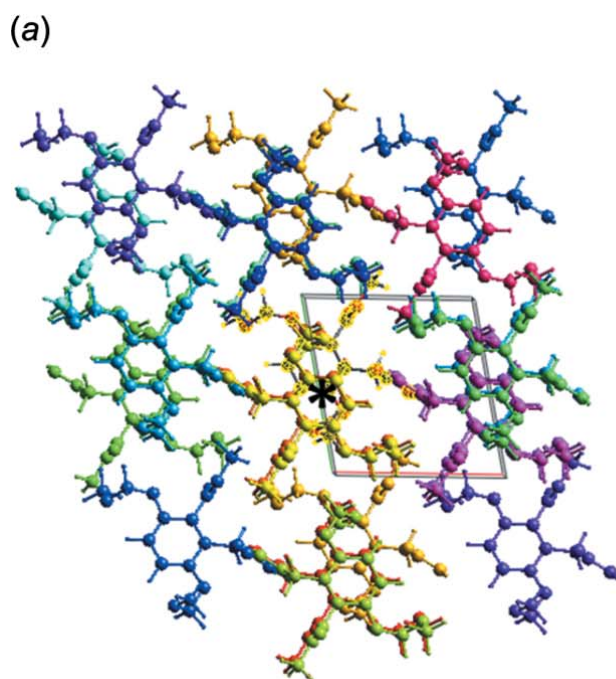

Figure 7

The energy frameworks for **I** viewed down the *c*-axis direction comprising, (a) electrostatic potential forces (E_{ele}), (b) dispersion forces (E_{dis}) and (c) total (E_{tot}) energy for a cluster about a reference molecule of **I**. The energy frameworks were adjusted to the same scale factor of 80 with a cut-off value of 5 kJ mol^{-1} within a 5 \AA radius of a selected central molecule.

confirmed by the two-dimensional fingerprint plots (Fig. 6). The principal intermolecular contacts for **I** are delineated into $\text{H}\cdots\text{H}$ (48.0%) (Fig. 6b), $\text{O}\cdots\text{H}/\text{H}\cdots\text{O}$ (41.1%) (Fig. 6c), $\text{C}\cdots\text{H}/\text{H}\cdots\text{C}$ (7.2%) (Fig. 6d) and $\text{C}\cdots\text{C}$ (2.7%) (Fig. 6e) contacts. The intermolecular contacts are therefore almost equally distributed between electrostatic and dispersion forces, as shown in Fig. 7a and 7b. The energy frameworks (Fig. 7) were adjusted to the same scale factor of 80 with a cut-off value of 5 kJ mol^{-1} within a radius of 5 \AA about a central

molecule, and were obtained using the wave function calculated at the HF/3-21G level of theory.

The calculation of the energy framework results in a colour-coded molecular cluster related to the specific interaction energy, see Fig. 8a. The individual energy components, electrostatic (E_{ele}), polarization (E_{pol}), dispersion (E_{dis}) and repulsion (E_{rep}) energies and the sum of these components (E_{tot}) for the interactions relative to a reference molecule (*) are shown in Fig. 8b.


(b)

	N	Symp	R	Electron Density	E_{ele}	E_{pol}	E_{dis}	E_{rep}	E_{tot}
	1	-x, -y, -z	11.24	HF/3-21G	2.6	-0.5	-4.0	0.4	-0.9
	1	-x, -y, -z	4.62	HF/3-21G	-30.4	-13.4	-75.6	44.4	-71.8
	2	x, y, z	9.66	HF/3-21G	-12.1	-4.0	-28.8	16.3	-27.7
	1	-x, -y, -z	6.76	HF/3-21G	0.4	-6.6	-44.4	21.9	-26.1
	1	-x, -y, -z	14.98	HF/3-21G	-0.1	-0.0	-0.6	0.0	-0.7
	1	-x, -y, -z	10.37	HF/3-21G	0.9	-0.2	-5.1	0.2	-3.6
	2	x, y, z	12.60	HF/3-21G	-1.5	-0.1	-0.8	0.0	-2.3
	1	-x, -y, -z	10.16	HF/3-21G	-8.5	-4.5	-10.6	2.6	-19.0
	1	-x, -y, -z	14.57	HF/3-21G	1.3	-0.3	-4.8	2.6	-1.1
	2	x, y, z	8.56	HF/3-21G	-14.4	-3.9	-28.2	15.0	-30.5
	2	x, y, z	11.99	HF/3-21G	-1.4	-0.1	-1.8	0.0	-3.2
	1	-x, -y, -z	7.32	HF/3-21G	-15.8	-3.4	-18.2	4.1	-31.4
	2	x, y, z	13.77	HF/3-21G	0.4	-0.1	-1.0	0.0	-0.5
	1	-x, -y, -z	9.05	HF/3-21G	1.0	-0.2	-3.7	0.0	-2.4
	1	-x, -y, -z	9.59	HF/3-21G	-113.7	-37.4	-17.1	100.2	-74.4
	1	-x, -y, -z	8.77	HF/3-21G	-13.9	-5.9	-25.0	14.4	-28.9

Figure 8

The colour-coding interaction mapping within 5 \AA of the centering (*) molecular cluster.

Table 3

 Selected torsion angles ($^{\circ}$) in compound **I** compared to those in compounds GEZPUZ, GEZQAG and IVIQIP.

I	
C3–O3–C9–O4	–77.8 (2)
C10–O4–C9–O3	–67.6 (2)
C6–O5–C11–O6	–61.3 (2)
C12–O6–C11–O5	–65.5 (2)
GEZPUZ ^a	
C7–O4–C13–O1	67.1 (3)
C16–O1–C13–O4	56.3 (3)
C8–O5–C12–O6	–80.1 (2)
C17–O6–C12–O5	–65.8 (3)
GEZQAG ^a	
C7–O2–C12–O7	–71.2 (8)
C16–O7–C12–O2	–67.6 (9)
C9–O3–C10–O6	86.1 (7)
C17–O6–C10–O3	76.6 (8)
IVIQIP ^{b,c}	
C1–O1–C8–O2	–68.9 (2)
C9–O2–C8–O1	–66.1 (2)

(a) Nakayama *et al.* (2018); (b) Zhang *et al.* (2017); (c) compound IVIQIP possesses inversion symmetry.

5. Database survey

A search of the Cambridge Structural Database (CSD, Version 5.41, last update March 2020; Groom *et al.*, 2016) for the 3,6-bis(methoxymethoxy)phenyl substructure gave only six hits. Three compounds are of particular interest, namely 1-[2-bromo-3,6-bis(methoxymethoxy)phenyl]-1-methoxyheptan-2-ol (CSD refcode GEZPUZ; Nakayama *et al.*, 2018), 7-bromo-4-methoxy-5,8-bis(methoxymethoxy)-3-pentyl-3,4-dihydro-1*H*-2-benzopyran-1-one (GEZQAG; Nakayama *et al.*, 2018) and 2,2'-[[2,5-bis(methoxymethoxy)-1,4-phenylene]dimethylidene]dimalononitrile (IVIQIP; Zhang *et al.*, 2017). The first two, GEZPUZ and GEZQAG [compounds 17 and 20 in the publication by Nakayama *et al.* (2018)], are key intermediates in the synthesis of the dihydroisocoumarin-type natural products, eurtiumide A and eurtiumide B. Compound IVIQIP [compound 1c in the publication by Zhang *et al.* (2017)] was synthesized in a study of organic solid fluorophores. The conformation of the –O–CH₂–O–CH₃ side chains are compared to that in compound **I** in Fig. 9 and Table 3. In GEZPUZ and GEZQAG these side chains are twisted and directed to the same side of the benzene ring. In IVIQIP they are also twisted but directed to opposite sides of the benzene ring as in compound **I**.

A search of the CSD for the substructure 2-(2-(methoxycarbonyl)phenyl)acetic acid gave zero hits.

6. Synthesis and crystallization

The synthesis of compound **I** is illustrated in Fig. 1. Full details of the syntheses and spectroscopic and analytical data for compounds **2–5** and **I** are available in the PhD thesis of Tiouabi (2005). It can be downloaded from the website <https://doc.rero.ch/record>, a digital library where many theses of

Swiss universities are deposited. Colourless block-like crystals of **I** were obtained by slow evaporation of a solution in acetone-*d*₆.

7. Refinement

Crystal data, data collection and structure refinement details are summarized in Table 4. The OH and C-bound H atoms were included in calculated positions and treated as riding atoms: O–H = 0.84 Å, C–H = 0.95–0.99 Å with $U_{iso}(H) = 1.5U_{eq}(OH \text{ and C-methyl})$ and $1.2U_{eq}(C)$ for other H-atoms.

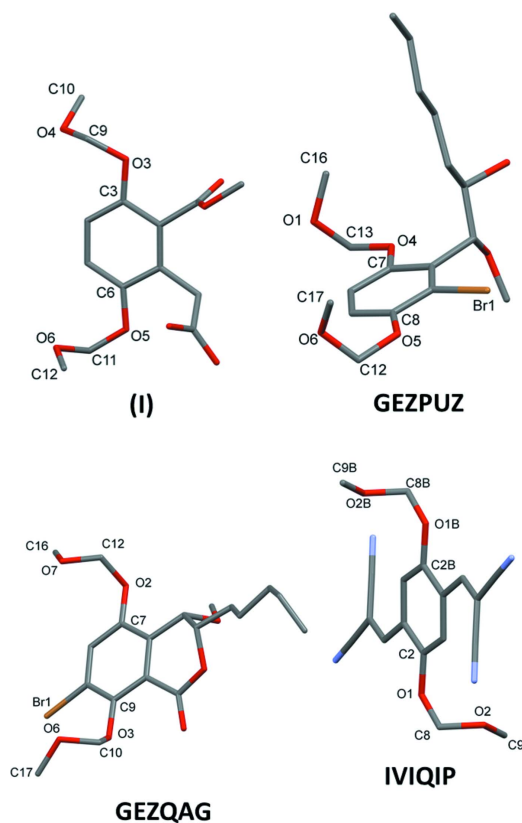
Intensity data were measured using a Stoe IPDS I, a one-circle diffractometer. For the triclinic system often only 93% of the Ewald sphere is accessible, which explains why the alert diffn_reflns_laue_measured_fraction_full value (0.942) below minimum (0.95) is given. This involves 155 random reflections out of the expected 2692 for the IUCr cutoff limit of $\sin \theta/\lambda = 0.60$.

Acknowledgements

RT and HSE are grateful to the University of Neuchâtel for their support over the years.

Funding information

Funding for this research was provided by: Swiss National Science Foundation and the University of Neuchâtel.


Figure 9

A view of the molecular structures of **I**, GEZPUZ, GEZQAG and IVIQIP. The original atom-labelling schemes have been used for the latter three compounds. For clarity, H atoms have been omitted

Table 4
Experimental details.

Crystal data	
Chemical formula	C ₁₄ H ₁₈ O ₈
<i>M</i> _r	314.28
Crystal system, space group	Triclinic, <i>P</i> $\bar{1}$
Temperature (K)	173
<i>a</i> , <i>b</i> , <i>c</i> (Å)	8.5628 (12), 9.6623 (13), 9.9767 (12)
α , β , γ (°)	112.534 (14), 94.744 (15), 97.999 (16)
<i>V</i> (Å ³)	746.60 (19)
<i>Z</i>	2
Radiation type	Mo <i>K</i> α
μ (mm ⁻¹)	0.12
Crystal size (mm)	0.30 × 0.30 × 0.20
Data collection	
Diffractometer	Stoe IPDS 1
Absorption correction	Multi-scan (<i>MULABS</i> ; Spek, 2020)
<i>T</i> _{min} , <i>T</i> _{max}	0.827, 1.000
No. of measured, independent and observed [<i>I</i> > 2 σ (<i>I</i>)] reflections	6011, 2752, 1557
<i>R</i> _{int}	0.065
(<i>sin</i> θ / λ) _{max} (Å ⁻¹)	0.617
Refinement	
<i>R</i> [<i>F</i> ² > 2 σ (<i>F</i> ²)], <i>wR</i> (<i>F</i> ²), <i>S</i>	0.045, 0.108, 0.83
No. of reflections	2752
No. of parameters	204
H-atom treatment	H-atom parameters constrained
$\Delta\rho_{\max}$, $\Delta\rho_{\min}$ (e Å ⁻³)	0.25, -0.23

Computer programs: *EXPOSE*, *CELL* and *INTEGRATE* in *IPDS-I* (Stoe & Cie, 2004), *SHELXS97* (Sheldrick, 2008), *Mercury* (Macrae *et al.*, 2020), *SHELXL2018/3* (Sheldrick, 2015), *PLATON* (Spek, 2020) and *publCIF* (Westrip, 2010).

References

- Bürki, N., Michel, A. & Tabacchi, R. (2003). *Phytopathol. Mediterr.* **42**, 191–198.
- Gremaud, G. & Tabacchi, R. (1994). *Nat. Prod. Lett.* **5**, 95–103.
- Groom, C. R., Bruno, I. J., Lightfoot, M. P. & Ward, S. C. (2016). *Acta Cryst.* **B72**, 171–179.
- Macrae, C. F., Sovago, I., Cottrell, S. J., Galek, P. T. A., McCabe, P., Pidcock, E., Platings, M., Shields, G. P., Stevens, J. S., Towler, M. & Wood, P. A. (2020). *J. Appl. Cryst.* **53**, 226–235.
- McKinnon, J. J., Jayatilaka, D. & Spackman, M. A. (2007). *Chem. Commun.* pp. 3814.
- Michel, A. (2001). PhD Thesis. University of Neuchâtel, Switzerland.
- Nakayama, A., Sata, H., Karanjit, S., Hayashi, N., Oda, M. & Namba, K. (2018). *Eur. J. Org. Chem.* pp. 4013–4017.
- Sheldrick, G. M. (2008). *Acta Cryst.* **A64**, 112–122.
- Sheldrick, G. M. (2015). *Acta Cryst.* **C71**, 3–8.
- Spackman, M. A. & Jayatilaka, D. (2009). *CrystEngComm*, **11**, 19–32.
- Spek, A. L. (2020). *Acta Cryst.* **E76**, 1–11.
- Stoe & Cie (2004). *IPDSI Bedienungshandbuch*. Stoe & Cie GmbH, Darmstadt, Germany.
- Tan, S. L., Jotani, M. M. & Tiekink, E. R. T. (2019). *Acta Cryst.* **E75**, 308–318.
- Tiouabi, M. (2001). PhD Thesis. University of Neuchâtel, Switzerland. Available from <https://doc.rero.ch/record>
- Turner, M. J., McKinnon, J. J., Wolff, S. K., Grimwood, D. J., Spackman, P. R., Jayatilaka, D. & Spackman, M. A. (2017). *CrystalExplorer17*. University of Western Australia. <http://hirshfeldsurface.net>
- Turner, M. J., Thomas, S. P., Shi, M. W., Jayatilaka, D. & Spackman, M. A. (2015). *Chem. Commun.* **51**, 3735–3738.
- Westrip, S. P. (2010). *J. Appl. Cryst.* **43**, 920–925.
- Zhang, J. N., Kang, H., Li, N., Zhou, S. M., Sun, H. M., Yin, S. W., Zhao, N. & Tang, B. Z. (2017). *Chem. Sci.* **8**, 577–582.

supporting information

Acta Cryst. (2020). E76, 1101-1106 [https://doi.org/10.1107/S2056989020007987]

The crystal structure, Hirshfeld surface analysis and energy frameworks of 2-[2-(methoxycarbonyl)-3,6-bis(methoxymethoxy)phenyl]acetic acid

Mustapha Tiouabi, Raphaël Tabacchi and Helen Stoeckli-Evans

Computing details

Data collection: *EXPOSE* in *IPDS-I* (Stoe & Cie, 2004); cell refinement: *CELL* in *IPDS-I* (Stoe & Cie, 2004); data reduction: *INTEGRATE* in *IPDS-I* (Stoe & Cie, 2004); program(s) used to solve structure: *SHELXS97* (Sheldrick, 2008); program(s) used to refine structure: *SHELXL2018/3* (Sheldrick, 2015); molecular graphics: *Mercury* (Macrae *et al.*, 2020); software used to prepare material for publication: *SHELXL2018/3* (Sheldrick, 2015), *PLATON* (Spek, 2020) and *publCIF* (Westrip, 2010).

2-[2-(Methoxycarbonyl)-3,6-bis(methoxymethoxy)phenyl]acetic acid

Crystal data

$C_{14}H_{18}O_8$	$Z = 2$
$M_r = 314.28$	$F(000) = 332$
Triclinic, $P\bar{1}$	$D_x = 1.398 \text{ Mg m}^{-3}$
$a = 8.5628 (12) \text{ \AA}$	Mo $K\alpha$ radiation, $\lambda = 0.71073 \text{ \AA}$
$b = 9.6623 (13) \text{ \AA}$	Cell parameters from 3063 reflections
$c = 9.9767 (12) \text{ \AA}$	$\theta = 2.2\text{--}25.8^\circ$
$\alpha = 112.534 (14)^\circ$	$\mu = 0.12 \text{ mm}^{-1}$
$\beta = 94.744 (15)^\circ$	$T = 173 \text{ K}$
$\gamma = 97.999 (16)^\circ$	Block, colourless
$V = 746.60 (19) \text{ \AA}^3$	$0.30 \times 0.30 \times 0.20 \text{ mm}$

Data collection

Stoe IPDS 1	6011 measured reflections
diffractometer	2752 independent reflections
Radiation source: fine-focus sealed tube	1557 reflections with $I > 2\sigma(I)$
Plane graphite monochromator	$R_{\text{int}} = 0.065$
φ rotation scans	$\theta_{\text{max}} = 26.0^\circ$, $\theta_{\text{min}} = 2.3^\circ$
Absorption correction: multi-scan	$h = -10 \rightarrow 10$
(MULABS; Spek, 2020)	$k = -11 \rightarrow 11$
$T_{\text{min}} = 0.827$, $T_{\text{max}} = 1.000$	$l = -11 \rightarrow 11$

Refinement

Refinement on F^2	0 restraints
Least-squares matrix: full	Primary atom site location: structure-invariant direct methods
$R[F^2 > 2\sigma(F^2)] = 0.045$	Secondary atom site location: difference Fourier map
$wR(F^2) = 0.108$	Hydrogen site location: inferred from neighbouring sites
$S = 0.83$	
2752 reflections	
204 parameters	

H-atom parameters constrained

$$w = 1/[\sigma^2(F_o^2) + (0.0527P)^2]$$

$$\text{where } P = (F_o^2 + 2F_c^2)/3$$

$$(\Delta/\sigma)_{\max} < 0.001$$

$$\Delta\rho_{\max} = 0.25 \text{ e } \text{\AA}^{-3}$$

$$\Delta\rho_{\min} = -0.23 \text{ e } \text{\AA}^{-3}$$

Extinction correction: (SHELXL2018/3;
Sheldrick, 2015),

$$F_c^* = kFc[1 + 0.001x\lambda^3/\sin(2\theta)]^{-1/4}$$

Extinction coefficient: 0.019 (5)

Special details

Geometry. All esds (except the esd in the dihedral angle between two l.s. planes) are estimated using the full covariance matrix. The cell esds are taken into account individually in the estimation of esds in distances, angles and torsion angles; correlations between esds in cell parameters are only used when they are defined by crystal symmetry. An approximate (isotropic) treatment of cell esds is used for estimating esds involving l.s. planes.

Fractional atomic coordinates and isotropic or equivalent isotropic displacement parameters (Å²)

	<i>x</i>	<i>y</i>	<i>z</i>	<i>U</i> _{iso} */ <i>U</i> _{eq}
O1	0.25754 (19)	0.8960 (2)	0.1239 (2)	0.0457 (5)
O2	0.30589 (19)	0.94409 (18)	0.3608 (2)	0.0427 (5)
O3	-0.08148 (17)	0.86702 (16)	0.21564 (19)	0.0354 (4)
O4	-0.36196 (18)	0.82093 (18)	0.1605 (2)	0.0411 (5)
O5	0.12039 (17)	0.34010 (16)	0.18992 (18)	0.0313 (4)
O6	-0.07328 (18)	0.23819 (17)	0.29737 (19)	0.0357 (4)
O7	0.35707 (18)	0.58696 (18)	0.45712 (19)	0.0373 (4)
O8	0.52484 (19)	0.4650 (2)	0.3133 (2)	0.0449 (5)
H8	0.548084	0.441888	0.384533	0.067*
C1	0.1715 (2)	0.5912 (2)	0.2067 (2)	0.0255 (5)
C2	0.1204 (2)	0.7231 (2)	0.2130 (2)	0.0255 (5)
C3	-0.0431 (2)	0.7295 (2)	0.2044 (3)	0.0266 (5)
C4	-0.1531 (2)	0.6025 (2)	0.1876 (3)	0.0290 (5)
H4	-0.263625	0.606043	0.179939	0.035*
C5	-0.1034 (2)	0.4714 (2)	0.1817 (3)	0.0292 (5)
H5	-0.179938	0.384882	0.170246	0.035*
C6	0.0580 (2)	0.4643 (2)	0.1925 (2)	0.0262 (5)
C7	0.2333 (2)	0.8614 (2)	0.2243 (3)	0.0284 (5)
C8	0.4160 (3)	1.0825 (3)	0.3806 (3)	0.0494 (7)
H8A	0.495875	1.056174	0.314572	0.074*
H8B	0.469429	1.131775	0.482449	0.074*
H8C	0.356664	1.152557	0.357997	0.074*
C9	-0.2285 (3)	0.8986 (3)	0.2679 (3)	0.0376 (6)
H9A	-0.238127	0.869474	0.352219	0.045*
H9B	-0.226769	1.009573	0.303253	0.045*
C10	-0.3713 (3)	0.8721 (3)	0.0443 (3)	0.0509 (7)
H10A	-0.362356	0.983164	0.085357	0.076*
H10B	-0.473812	0.824240	-0.019781	0.076*
H10C	-0.284222	0.844062	-0.012623	0.076*
C11	0.0113 (3)	0.2090 (2)	0.1794 (3)	0.0314 (5)
H11A	-0.065027	0.172092	0.087538	0.038*
H11B	0.071162	0.126917	0.174037	0.038*
C12	0.0227 (3)	0.2754 (3)	0.4335 (3)	0.0487 (7)
H12A	0.078802	0.191711	0.426820	0.073*

H12B	-0.044987	0.291178	0.510676	0.073*
H12C	0.100661	0.368863	0.457137	0.073*
C13	0.3446 (2)	0.5742 (3)	0.2107 (3)	0.0313 (6)
H13A	0.356492	0.490502	0.118404	0.038*
H13B	0.409856	0.669321	0.215295	0.038*
C14	0.4080 (2)	0.5412 (2)	0.3378 (3)	0.0305 (5)

Atomic displacement parameters (Å²)

	U^{11}	U^{22}	U^{33}	U^{12}	U^{13}	U^{23}
O1	0.0385 (9)	0.0556 (11)	0.0457 (13)	-0.0099 (8)	-0.0036 (8)	0.0315 (9)
O2	0.0435 (10)	0.0378 (9)	0.0348 (12)	-0.0124 (7)	-0.0001 (8)	0.0095 (8)
O3	0.0246 (8)	0.0319 (8)	0.0551 (13)	0.0073 (7)	0.0093 (7)	0.0217 (8)
O4	0.0259 (8)	0.0473 (10)	0.0627 (14)	0.0081 (7)	0.0063 (8)	0.0351 (9)
O5	0.0300 (8)	0.0276 (8)	0.0384 (11)	0.0054 (6)	0.0041 (7)	0.0156 (7)
O6	0.0350 (9)	0.0405 (9)	0.0339 (12)	0.0031 (7)	0.0048 (7)	0.0189 (8)
O7	0.0339 (9)	0.0460 (9)	0.0320 (12)	0.0076 (7)	0.0029 (8)	0.0159 (8)
O8	0.0354 (9)	0.0633 (11)	0.0482 (14)	0.0216 (8)	0.0067 (8)	0.0311 (10)
C1	0.0224 (10)	0.0305 (11)	0.0229 (14)	0.0026 (9)	0.0015 (9)	0.0112 (9)
C2	0.0245 (11)	0.0282 (11)	0.0243 (15)	0.0007 (9)	0.0016 (9)	0.0127 (9)
C3	0.0269 (11)	0.0283 (11)	0.0281 (15)	0.0075 (9)	0.0032 (9)	0.0144 (10)
C4	0.0219 (11)	0.0340 (12)	0.0320 (16)	0.0036 (9)	0.0019 (9)	0.0151 (10)
C5	0.0239 (11)	0.0299 (12)	0.0312 (15)	-0.0015 (9)	0.0006 (9)	0.0123 (10)
C6	0.0266 (11)	0.0283 (11)	0.0248 (15)	0.0060 (9)	0.0022 (9)	0.0118 (10)
C7	0.0233 (11)	0.0333 (12)	0.0313 (16)	0.0057 (9)	0.0019 (10)	0.0161 (11)
C8	0.0392 (14)	0.0377 (14)	0.055 (2)	-0.0118 (11)	0.0019 (13)	0.0082 (12)
C9	0.0320 (12)	0.0371 (13)	0.0486 (19)	0.0120 (10)	0.0119 (11)	0.0191 (12)
C10	0.0426 (15)	0.0641 (17)	0.060 (2)	0.0190 (13)	0.0137 (13)	0.0355 (15)
C11	0.0370 (13)	0.0257 (11)	0.0293 (16)	0.0006 (9)	0.0014 (10)	0.0111 (10)
C12	0.0506 (16)	0.0578 (17)	0.0354 (19)	0.0046 (13)	0.0034 (12)	0.0187 (13)
C13	0.0237 (11)	0.0346 (12)	0.0395 (17)	0.0064 (9)	0.0054 (10)	0.0186 (11)
C14	0.0206 (11)	0.0317 (12)	0.0389 (18)	0.0009 (9)	0.0013 (10)	0.0158 (11)

Geometric parameters (Å, °)

O1—C7	1.196 (3)	C4—C5	1.374 (3)
O2—C7	1.329 (3)	C4—H4	0.9500
O2—C8	1.461 (3)	C5—C6	1.391 (3)
O3—C3	1.379 (2)	C5—H5	0.9500
O3—C9	1.429 (3)	C8—H8A	0.9800
O4—C9	1.400 (3)	C8—H8B	0.9800
O4—C10	1.425 (3)	C8—H8C	0.9800
O5—C6	1.372 (2)	C9—H9A	0.9900
O5—C11	1.429 (2)	C9—H9B	0.9900
O6—C11	1.390 (3)	C10—H10A	0.9800
O6—C12	1.417 (3)	C10—H10B	0.9800
O7—C14	1.240 (3)	C10—H10C	0.9800
O8—C14	1.308 (3)	C11—H11A	0.9900

O8—H8	0.8400	C11—H11B	0.9900
C1—C2	1.386 (3)	C12—H12A	0.9800
C1—C6	1.408 (3)	C12—H12B	0.9800
C1—C13	1.513 (3)	C12—H12C	0.9800
C2—C3	1.406 (3)	C13—C14	1.499 (3)
C2—C7	1.496 (3)	C13—H13A	0.9900
C3—C4	1.383 (3)	C13—H13B	0.9900
C7—O2—C8	115.27 (19)	O4—C9—O3	113.0 (2)
C3—O3—C9	116.23 (16)	O4—C9—H9A	109.0
C9—O4—C10	113.21 (19)	O3—C9—H9A	109.0
C6—O5—C11	117.44 (16)	O4—C9—H9B	109.0
C11—O6—C12	113.99 (18)	O3—C9—H9B	109.0
C14—O8—H8	109.5	H9A—C9—H9B	107.8
C2—C1—C6	119.14 (18)	O4—C10—H10A	109.5
C2—C1—C13	123.33 (18)	O4—C10—H10B	109.5
C6—C1—C13	117.51 (18)	H10A—C10—H10B	109.5
C1—C2—C3	120.27 (18)	O4—C10—H10C	109.5
C1—C2—C7	122.31 (18)	H10A—C10—H10C	109.5
C3—C2—C7	117.40 (18)	H10B—C10—H10C	109.5
O3—C3—C4	124.46 (18)	O6—C11—O5	112.89 (17)
O3—C3—C2	115.83 (17)	O6—C11—H11A	109.0
C4—C3—C2	119.71 (18)	O5—C11—H11A	109.0
C5—C4—C3	120.44 (19)	O6—C11—H11B	109.0
C5—C4—H4	119.8	O5—C11—H11B	109.0
C3—C4—H4	119.8	H11A—C11—H11B	107.8
C4—C5—C6	120.48 (18)	O6—C12—H12A	109.5
C4—C5—H5	119.8	O6—C12—H12B	109.5
C6—C5—H5	119.8	H12A—C12—H12B	109.5
O5—C6—C5	125.22 (17)	O6—C12—H12C	109.5
O5—C6—C1	114.84 (17)	H12A—C12—H12C	109.5
C5—C6—C1	119.94 (19)	H12B—C12—H12C	109.5
O1—C7—O2	122.7 (2)	C14—C13—C1	113.74 (19)
O1—C7—C2	125.0 (2)	C14—C13—H13A	108.8
O2—C7—C2	112.25 (19)	C1—C13—H13A	108.8
O2—C8—H8A	109.5	C14—C13—H13B	108.8
O2—C8—H8B	109.5	C1—C13—H13B	108.8
H8A—C8—H8B	109.5	H13A—C13—H13B	107.7
O2—C8—H8C	109.5	O7—C14—O8	123.2 (2)
H8A—C8—H8C	109.5	O7—C14—C13	122.6 (2)
H8B—C8—H8C	109.5	O8—C14—C13	114.1 (2)
C6—C1—C2—C3	-0.3 (3)	C13—C1—C6—O5	2.6 (3)
C13—C1—C2—C3	178.2 (2)	C2—C1—C6—C5	1.4 (3)
C6—C1—C2—C7	-178.5 (2)	C13—C1—C6—C5	-177.2 (2)
C13—C1—C2—C7	0.0 (3)	C8—O2—C7—O1	1.1 (3)
C9—O3—C3—C4	24.5 (3)	C8—O2—C7—C2	-178.97 (19)
C9—O3—C3—C2	-154.8 (2)	C1—C2—C7—O1	99.6 (3)

C1—C2—C3—O3	178.31 (19)	C3—C2—C7—O1	-78.6 (3)
C7—C2—C3—O3	-3.4 (3)	C1—C2—C7—O2	-80.3 (3)
C1—C2—C3—C4	-1.0 (3)	C3—C2—C7—O2	101.5 (2)
C7—C2—C3—C4	177.3 (2)	C10—O4—C9—O3	-67.6 (2)
O3—C3—C4—C5	-178.0 (2)	C3—O3—C9—O4	-77.8 (2)
C2—C3—C4—C5	1.2 (3)	C12—O6—C11—O5	-65.5 (2)
C3—C4—C5—C6	-0.1 (3)	C6—O5—C11—O6	-61.3 (2)
C11—O5—C6—C5	-1.9 (3)	C2—C1—C13—C14	119.8 (2)
C11—O5—C6—C1	178.44 (19)	C6—C1—C13—C14	-61.7 (3)
C4—C5—C6—O5	179.1 (2)	C1—C13—C14—O7	-29.8 (3)
C4—C5—C6—C1	-1.2 (3)	C1—C13—C14—O8	152.52 (19)
C2—C1—C6—O5	-178.9 (2)		

Hydrogen-bond geometry (\AA , $^\circ$)

Cg is the centroid of the C1–C6 benzene ring.

<i>D</i> —H \cdots <i>A</i>	<i>D</i> —H	H \cdots <i>A</i>	<i>D</i> \cdots <i>A</i>	<i>D</i> —H \cdots <i>A</i>
C4—H4 \cdots O4	0.95	2.41	3.022 (3)	122
O8—H8 \cdots O7 ⁱ	0.84	1.85	2.676 (2)	168
C9—H9 <i>B</i> \cdots O6 ⁱⁱ	0.99	2.43	3.256 (3)	140
C11—H11 <i>A</i> \cdots O1 ⁱⁱⁱ	0.99	2.38	3.366 (3)	175
C13—H13 <i>B</i> \cdots O4 ^{iv}	0.99	2.50	3.421 (3)	155
C12—H12 <i>B</i> \cdots <i>Cg</i> ^v	0.98	2.66	3.451 (3)	138

Symmetry codes: (i) $-x+1, -y+1, -z+1$; (ii) $x, y+1, z$; (iii) $-x, -y+1, -z$; (iv) $x+1, y, z$; (v) $-x, -y+1, -z+1$.